International Immunology, Vol. 32, No. 8, pp. 559–568
doi:10.1093/intimm/dxaa029
Advance Access publication 29 April 2020

Impaired mucociliary motility enhances antigen-specific nasal IgA immune responses to a cholera toxin-based nasal vaccine

Huangwenxian Lan[1,2], Hidehiko Suzuki[1], Takahiro Nagatake[1], Koji Hosomi[1], Koji Ikegami[3], Mitsutoshi Setou[4] and **Jun Kunisawa[1,2,5,6,7]**

[1]Laboratory of Vaccine Materials, Center for Vaccine and Adjuvant Research and Laboratory of Gut Environmental System, National Institutes of Biomedical Innovation, Health and Nutrition (NIBIOHN), Osaka 567-0085, Japan
[2]Graduate School of Pharmaceutical Sciences, Osaka University, Osaka 565-0871, Japan
[3]Graduate School of Biomedical & Health Sciences, Hiroshima University, Hiroshima 734-8553, Japan
[4]Department of Cellular & Molecular Anatomy, Hamamatsu University School of Medicine, Shizuoka 431-3192, Japan
[5]International Research and Development Center for Mucosal Vaccines, The Institute of Medical Science, University of Tokyo, Tokyo 108-0071, Japan
[6]Graduate School of Medicine, Kobe University, Hyogo 650-0017, Japan
[7]Graduate School of Medicine and Graduate School of Dentistry, Osaka University, Osaka 565-0871, Japan

Correspondence to: J. Kunisawa; E-mail: kunisawa@nibiohn.go.jp

Received 9 November 2019, *editorial decision* 16 April 2020; *accepted* 24 April 2020

Abstract

Nasal mucosal tissues are equipped with physical barriers, mucus and cilia, on their surface. The mucus layer captures inhaled materials, and the cilia remove the inhaled materials from the epithelial layer by asymmetrical beating. The effect of nasal physical barriers on the vaccine efficacy remains to be investigated. Tubulin tyrosine ligase-like family, member 1 (Ttll1) is an essential enzyme for appropriate movement of the cilia on respiratory epithelium, and its deficiency (Ttll1-KO) leads to mucus accumulation in the nasal cavity. Here, when mice were intra-nasally immunized with pneumococcal surface protein A (PspA, as vaccine antigen) together with cholera toxin (CT, as mucosal adjuvant), Ttll1-KO mice showed higher levels of PspA-specific IgA in the nasal wash and increased numbers of PspA-specific IgA-producing plasma cells in the nasal passages when compared with Ttll1 hetero (He) mice. Mucus removal by *N*-acetylcysteine did not affect the enhanced immune responses in Ttll1-KO mice versus Ttll1-He mice. Immunohistological and flow cytometry analyses revealed that retention time of PspA in the nasal cavity in Ttll1-KO mice was longer than that in Ttll1-He mice. Consistently, uptake of PspA by dendritic cells was higher in the nasopharynx-associated lymphoid tissue (NALT) of Ttll1-KO mice than that of Ttll1-He mice. These results indicate that the ciliary function of removing vaccine antigen from the NALT epithelial layer is a critical determinant of the efficacy of nasal vaccine.

Keywords: ciliary movement, immunity, mucus, NALT, Ttll1

Introduction

Mucosa separates our inner body from the outside environment, and the mucosal surface is continually exposed to exogenous materials. Most pathogens invade our body through mucosal tissues, including the eye, respiratory tract, intestine and genital tract, and the mucosal immune system forms the first line of defense. Secretory IgA plays an important role in preventing the entry of pathogens and neutralizing toxins (1). Mucosal vaccines such as nasal and oral vaccines can induce mucosal immune responses as well as systemic immune responses, which is ideal for preventing infectious diseases; thus, several mucosal vaccines are clinically used (2).

Mucosa-associated lymphoid tissues (MALTs), which develop at various mucosal surface sites in tear duct, nasal cavity and intestine, are important inductive sites for the antigen-specific mucosal IgA immune response (3). Nasopharynx-associated lymphoid tissue (NALT) is one of the MALTs in the nasal cavity. Antigens are taken up by M cells located on NALT epithelium (4). Antigen-presenting cells [APCs; e.g. dendritic cells (DCs)] in NALT capture the antigen

delivered by M cells and present it to T cells and B cells to initiate antigen-specific IgA immune responses (5–7). In nasal vaccines, delivery agents and adjuvant are widely applied to enhance antigen-specific IgA immune responses: delivery tools carry antigen to the NALT epithelium, which increases the antigen uptake by APCs (8), whereas adjuvant enhances the immune responses. Cholera toxin (CT) is frequently used as an experimental adjuvant because it strongly augments both humoral and cell-mediated immune responses (9). CT induces $CD4^+$ Th2 cells secreting interleukin (IL)-4, -5, -6 and -10 to provide helper signal for the induction of antigen-specific secretory IgA and serum IgG1, IgA and IgE antibody responses (10, 11). CT also promotes the differentiation of B cell into plasma cells (12).

In addition to providing an immunological barrier, mucosal tissues are equipped with physical barriers (i.e. mucus and mucocilia) on their surface as a part of their defense against foreign materials. Airway mucus secreted by goblet cells is composed of a network of high-molecular-weight glycoproteins that form a gel with properties of both a soft, elastic solid and a viscous fluid (13). Mucins, the main component of mucus, are classified into two broad classes: membrane-bound and secreted (14). Membrane-bound mucins are positioned in the plasma membrane, where they participate in such function as cellular adhesion, via their transmembrane and cytosolic domains and participate in other functions, including pathogen binding and signal transduction (15, 16); these proteins can be released into the extracellular mucous layer by proteolytic cleavage or alternative splicing (17). Structurally different from membrane-bound mucins, the secreted mucins contain cysteine-rich domains, which link covalently as disulfide bonds to form mucin dimers, and further multimerize to form the long linear oligomers that contribute to the properties of the mucus gel layer such as adhesion (13, 18). The airway mucus layer containing captured antigens is rapidly cleared by the asymmetrical beating of mucocilia, which are tail-like projections extending approximately outwards from the respiratory epithelia (19). Tubulin glutamylation, which adds several glutamic acids to the tubulin C-terminal tail domain to assemble the correct tubulin structure, is essential for ciliary function (20). The enzyme tubulin tyrosine ligase-like family, member 1 (Ttll1) has tubulin glutamylation activity, and the cilia of Ttll1 knockout (Ttll1-KO) mice lose beating asymmetry, leading to a significant accumulation of mucus in the nasal cavity (21).

Streptococcus pneumoniae is a major respiratory pathogen that causes pneumonia, otitis media and meningitis (22, 23). Selecting a vaccine antigen for this pathogen is challenging because there are over 90 *S. pneumoniae* serotypes, which differ by their polysaccharide capsule composition (24, 25). The current clinically used vaccine, which is based on conjugated pneumococcal polysaccharides, can only induce protective systemic immune responses against the covered serotypes, and does not induce protective mucosal immune responses because the vaccination is by intramuscular or subcutaneous injection (26). Moreover, after implementation of this polysaccharide-based vaccine, serotype replacement in both carriage and infection isolates has been observed (27) and the level of antibiotic resistance of the serotypes not contained in vaccine has increased (28). Thus, a pneumococcal vaccine with broader coverage and the ability to induce protective mucosal immune responses is clearly required. A recent study demonstrated that pneumococcal surface protein A (PspA) is an ideal vaccine antigen as it is produced by all *S. pneumoniae* with high antigenicity (29). Furthermore, in mouse studies, (i) administration of PspA-based nasal vaccines induces cross-protective immune responses in both systemic and respiratory mucosal compartments against the fatal infection of all strains of *S. pneumoniae* (30); (ii) PspA-specific serum IgG eliminates *S. pneumoniae* (31); and (iii) PspA-specific nasal IgA prevents streptococcal colonization of the nasal cavity (1, 32, 33).

Previously our group developed a claudin-4-targeted nasal vaccine by using the C-terminal fragment of *Clostridium perfringens* enterotoxin (C-CPE). Claudin-4 is expressed in the epithelium of NALT (34). We found that C-CPE fused with PspA (PspA-C-CPE) binds to NALT in a receptor-dependent fashion via claudin-4 and can induce effective PspA-specific nasal IgA immune responses (32). However, a failure of effective IgA production was found when Ttll1-KO mice were intra-nasally immunized with PspA-C-CPE, because the antigen binding to NALT was interrupted by dense mucus; the impaired efficacy of PspA-C-CPE could be rescued by mucus removal (35), suggesting that accumulated nasal mucus interferes with the delivery of nasal vaccines. As more adjuvant-based nasal vaccines are developed for clinical use, the effect of nasal physical barriers on the adjuvant-based vaccine efficacy remains unclear.

Here, we evaluated the efficacy of nasal vaccine by using Ttll1-KO mice to reveal the effects of mucociliary function on the induction of mucosal immune responses induced using the mucosal adjuvant, CT.

Methods

Mice

Ttll1-KO mice (C57BL/6 background) were generated as previously described (21). Ttll1-heterozygous littermates (Ttll1-He) were used as a control because they show the comparable level of immunological responses as wild-type mice (35). All mice were housed under a 12:12-h light:dark cycle and had free access to food and water. All experiments were approved by the Animal Care and Use Committee of the National Institutes of Biomedical Innovation, Health, and Nutrition (Osaka, Japan) and were conducted in accordance with their guidelines.

PspA and CT

pET16b plasmid encoding PspA protein was prepared as previously described (32) and transfected into *Escherichia coli* strain BL21 (DE3) (Toyobo, Osaka, Japan). To induce recombinant protein production, isopropyl-β-D-thiogalactopyranoside (Nacalai Tesque, Kyoto, Japan) was added into the culture medium. The culture pellet was sonicated in buffer A [10 mM Tris-HCl (pH 8.0), 400 mM NaCl, 5 mM $MgCl_2$, 0.1 mM phenylmethylsulfonyl fluoride, 1 mM 2-mercaptoethanol and 10% glycerol]. After centrifugation, the supernatant was loaded onto a HiTrap HP column (GE Healthcare, Pittsburgh, PA, USA). Recombinant PspA was

eluted by using buffer A containing 100–500 mM imidazole. The eluted protein solution was exchanged with phosphate-buffered saline (PBS) by using a PD-10 column (GE Healthcare). The concentration of purified protein was measured by using a BCA protein assay kit (Life Technologies, Carlsbad, CA, USA). Purification of the recombinant protein was confirmed by using a NuPAGE electrophoresis system (Life Technologies) followed by staining with Coomassie brilliant blue.

Biotinylated PspA was prepared with an EZ-Link Micro Sulfo-NHS-Biotinylation Kit (Pierce Biotechnology, Rockford, IL, USA). In brief, 1 mg PspA protein in 1 ml of PBS was mixed with 44.75 μl of 10 mM Sulfo-NHS-Biotin solution and incubated on ice for 2 h. A Zeba Spin Desalting Column was placed into a 15-ml collection tube, centrifuged at 1000 × *g* for 2 min to remove the storage buffer, and then twice equilibrated by adding 2.5 ml of PBS to the resin bed and centrifuging 1000 × *g* for 2 min. The prepared column was then placed into a new 15-ml tube, protein sample was applied onto the center of the resin bed and centrifuged at 1000 × *g* for 2 min, and the flow-through solution containing the purified protein sample was collected. The concentration of purified protein was measured by using a BCA protein assay kit, and the biotinylated PspA was stored at –80°C until use.

Fluorescein-4-isothiocyanate-labeled PspA (FITC-PspA) was prepared by using a SureLINK FITC Labeling Kit (SeraCare Life Sciences, Milford, MA, USA) (33). In brief, 0.3 mg FITC in 75 μl *N,N*-dimethylformamide (DMF) was added into 4 ml of PspA (0.5 mg ml^{-1}) in 0.1 M carbonate-bicarbonate buffer (pH 9.6) and incubated with gentle agitation for 1 h at room temperature in darkness. The kit-supplied spin filter was used to remove the unconjugated FITC, and the protein was concentrated by centrifugation at 14 000 × *g* for 10 min. The buffer was exchanged with PBS and the concentration of purified protein was measured by using a BCA protein assay kit. The FITC-PspA was stored at –80°C until future use.

CT was purchased from List Biological Laboratories, Inc. (Campbell, CA, USA). Alexa Fluor 647-labeled CT (AF647-CT) was prepared by using an Alexa Fluor 647 Protein Labeling Kit (Molecular Probes, Eugene, OR, USA). In brief, 50 μl of 1 M bicarbonate solution (pH ~8.3) was added into 0.5 ml of CT (2 mg ml^{-1}, in PBS). The protein solution was transferred to a vial of reactive dye containing a magnetic stir bar and incubated with gentle agitation for 1 h at room temperature in darkness. The kit-supplied purification column was used to remove the unconjugated dye. The protein concentration was measured by using a BCA protein assay kit, and the AF647-CT was stored at –80°C until use.

Immunization

Mice were intra-nasally immunized with 5 μg of PspA and 0.3 μg of CT in 15 μl of PBS once weekly for 3 weeks. One week after the final immunization, blood was collected and left on ice for 30 min; serum was then collected by centrifugation at 3000 × *g* for 10 min at 4°C. Nasal wash was collected in 200 μl of 4°C PBS. Bronchoalveolar lavage fluid was collected in 1 ml of 4°C PBS. All samples were stored at –80°C until used for the enzyme-linked immune sorbent assay (ELISA).

To remove nasal mucus, 15 μg of *N*-acetylcysteine (Sigma-Aldrich, St Louis, MO, USA) in 10 μl of PBS was intra-nasally administered to mice as previously described (35). After 30 min, PspA and CT were intra-nasally administered to mice as described above.

Enzyme-linked immune sorbent assay

Nunc MaxiSorp flat-bottom 96-well plates (Thermo Fisher Scientific, Waltham, MA, USA) were coated with PspA (0.05 μg per well) or CT (0.5 μg per well) in PBS and incubated overnight at 4°C. The plates were then blocked with 1% bovine serum albumin (BSA) in 170 μl of PBS for 2 h at room temperature. After washing with PBS containing 0.05% Tween 20 (v/v, 0.05% T-PBS, 3 × 200 μl per well), the plates were incubated with 2-fold serially diluted nasal wash or serum samples in 1% BSA–0.05% T-PBS (w/v/v) for 2 h at room temperature. The plates were then washed with 0.05% T-PBS (3 × 200 μl per well) and treated with goat anti-mouse IgA or IgG conjugated with horseradish peroxidase (Southern Biotech, Birmingham, AL, USA) in 1% BSA–0.05% T-PBS for 1 h at room temperature. After a wash with 0.05% T-PBS (3 × 200 μl per well), PspA- or CT-specific antibodies were detected by adding 3,3′,5,5′-tetramethylbenzidine peroxide substrate into the wells and incubating for 2 min at room temperature. Then, 0.5 M HCl was added to stop the color reaction, and the optical density was measured at 450 nm as an index of color reaction progression.

Cell isolation

To isolate mononuclear cells, NALT was obtained from the upper jaw of the mice. NALT cells were isolated by gently rubbing the NALT sample with a needle under a stereoscopic microscope, as previously described (35). Mononuclear cells from nasal passages (NPs) were isolated by mechanical dissociation through a 70-μm nylon mesh.

Enzyme-linked immunospot

Enzyme-linked immunospot (ELISpot) plates (MSHAN45, Millipore, Burlington, MA, USA) were coated with PspA (0.05 μg per well) or CT (0.5 μg per well) and incubated overnight at 4°C. After washing with PBS (3 × 200 μl per well), the plates were blocked with 10% newborn calf serum (NCS; Equitech-Bio, Kerrville, TX, USA) in RPMI-1640 medium (Sigma-Aldrich) (v/v, 10% NCS–RPMI) for 30 min at 37°C in a 5% CO_2 incubator. Single cells isolated from NPs of mice were suspended in 1 ml of 10% NCS–RPMI (equivalent to 10^6 initial cells per ml), and 5-fold serial dilutions were performed in 10% NCS–RPMI down to a concentration of 8×10^3 cells per ml. Each cell suspension (100 μl per well) was added to the coated ELISpot plates and cultured for 4 h at 37°C in a 5% CO_2 incubator. Cells were removed from the plates by washing with PBS (3 × 200 μl per well) and then PBS containing 1% Tween 20 (v/v, 0.1% T-PBS, 3 × 200 μl per well). Then, each well was treated with 100 μl of goat anti-mouse IgA conjugated with horseradish peroxidase (1:1000 dilution in 0.1% T-PBS) overnight at 4°C in darkness. The plates were washed with PBS (6 × 200 μl per well), and then 100 μl per well amino ethyl carbazole (AEC, 0.33 mg ml^{-1}) was added.

To prepare fresh AEC solution, 10 mg ml^{-1} AEC in DMF was diluted 1:30 in 0.1 M acetic acid (pH 5.0) with 0.015% (v/v) hydrogen peroxide. The filtered AEC solution was added into each well for 30 min at room temperature in darkness. The plates were then rinsed with tap water and allowed to completely dry at room temperature. The number of spot-forming cells was counted by using a CTL S6 Analyzer with ImmunoSpot (version 5.0) and Immuno Capture (version 6.3) software (Cellular Technology Limited, Shaker Heights, OH, USA).

Histochemical analysis

Mice were intra-nasally immunized with 5 μg of biotinylated PspA and 0.3 μg of CT in 15 μl of PBS to examine the distribution of PspA and CT. At 30 min, 1 h and 12 h after administration, skin and soft tissues were removed from the head of each immunized mouse. The head was then embedded in Super Cryo Embedding Medium (Section-Lab, Hiroshima, Japan) and cut into 6-μm sections by using a cryostat. Frozen sections were fixed in 100% acetone for 1 min at 4°C. To prevent non-specific binding, sections were incubated with PBS containing 2% NCS (v/v, 2% NCS-PBS) for 30 min at room temperature. The sections were washed with PBS and then stained with primary antibodies overnight at 4°C. After another wash with PBS, the sections were stained with secondary antibody for 30 min at room temperature. Following another wash with PBS, the sections were stained with 4′,6-diamidino-2-phenylindole (DAPI) for 10 min at room temperature to visualize the nuclei. After a final wash with PBS, the sections were mounted in Fluoromount (Diagnostic BioSystems, Pleasanton, CA, USA) and observed by fluorescence microscopy (BZ-9000, Keyence, Osaka, Japan). Antibodies used for immunohistological analysis are as follows: biotinylated PspA was visualized by staining with AF488-conjugated streptavidin (Thermo Fisher Scientific; S32354; 1:200), or AF546-conjugated streptavidin (Thermo Fisher Scientific; S11225; 1:200). CT was visualized by staining with rabbit anti-CT subunit β (Abcam, Cambridge, UK; ab34992; 1:1000), followed by staining with secondary antibody AF647-conjugated goat anti-rabbit IgG (Thermo Fisher Scientific; A21245; 1:200). M cells were identified by staining with AF488-conjugated anti-mouse GP2 (Medical & Biological Laboratories, Nagoya, Japan; D278-A48; 1:200).

For whole-mount staining, murine palates were removed from Ttll1-He and -KO mice. The tissues were washed with PBS and were fixed in 4% paraformaldehyde phosphate buffer solution (Nacalai Tesque) for 3 h at 4°C. To prevent non-specific binding, tissues were incubated with RPMI-1640 containing 10% fetal bovine serum (Thermo Fisher Scientific) for 1 h at room temperature. The tissues were washed with PBS and then stained with rhodamine-conjugated UEA-1 (Ulex Europaeus Agglutinin 1; Vector Laboratories; Burlingame, CA, USA; 1:100) for 1 h on ice for the identification of M cells. Following another wash with PBS, the tissues were mounted in Fluoromount and observed by a Leica TCS SP8 laser scanning confocal microscopy (Leica Microsystem, Wetzlar, Germany).

Flow cytometric analysis

Mice were intra-nasally administered with 5 μg of FITC-PspA and 0.3 μg of AF647-CT in 15 μl of PBS to examine the antigen uptake of PspA and CT. Cells were isolated from NALT at 12 h after immunization. The cells were washed with 2% NCS-PBS and incubated with anti-CD16/32 monoclonal antibody (TruStain FcX; BioLegend, San Diego, CA, USA; 101320; dilution, 1:100) for 15 min at room temperature. After another wash with 2% NCS-PBS, the cells were stained with PE/Cy7-conjugated anti-mouse CD11c (BioLegend; catalog no. 117318; dilution, 1:200) for 30 min at 4°C. After another wash with 2% NCS-PBS, the cells were stained with 7-AAD (7-aminoactinomycin D; BioLegend; catalog no. 420404; dilution, 1:100) for 10 min at 4°C. After a final wash with 2% NCS-PBS, the cells were analyzed by flow cytometry (MACSQuant; Miltenyi Biotec, Auburn, CA, USA).

Data analysis

Data are expressed as means ± SEM. Statistical analyses were performed by using Welch's *t*-test or the non-parametric Mann–Whitney *U*-test. *P*-values less than 0.05 were deemed statistically significant.

Results

Increased levels of PspA-specific nasal IgA immune responses in Ttll1-KO mice

To examine whether airway mucociliary dysfunction affects the efficacy of adjuvant-based nasal vaccines, Ttll1 hetero (Ttll1-He) and Ttll1-KO mice were intra-nasally immunized with PspA plus CT as mucosal adjuvant. We found that the amount of PspA-specific nasal IgA was significantly higher in Ttll1-KO mice than in Ttll1-He mice (Fig. 1A, $P = 0.002$). Consistently, the number of PspA-specific IgA-producing plasma cells in the NPs was significantly higher in Ttll1-KO mice than in Ttll1-He mice (Fig. 1B, $P = 0.023$). It is reported that antigen-specific mucosal IgG also plays a role in the protective effect of PspA vaccine (36, 37). We found that the amount of PspA-specific IgG was not changed in bronchoalveolar lavage fluid of Ttll1-KO mice when compared with Ttll1-He mice (Supplementary Figure 1). Thus, cilia dysfunction caused by Ttll1 deficiency led to the augmented nasal IgA responses against the nasally administered antigen, PspA.

CT-specific nasal IgA immune responses were not changed in Ttll1-KO mice

CT potently enhances PspA-specific immune responses, i.e. acts as vaccine adjuvant, and acts as an antigen to induce CT-specific IgA immune responses. When we measured CT-specific IgA responses, unlike PspA-specific IgA responses, the amount of CT-specific IgA was comparable between Ttll1-He and -KO mice (Fig. 2A, $P = 0.95$). Also, the number of CT-specific IgA-producing plasma cells in the NPs were similar in Ttll1-He and -KO mice (Fig. 2B, $P = 0.18$). These results show that the CT-specific nasal IgA immune responses were not affected by the airway mucociliary dysfunction.

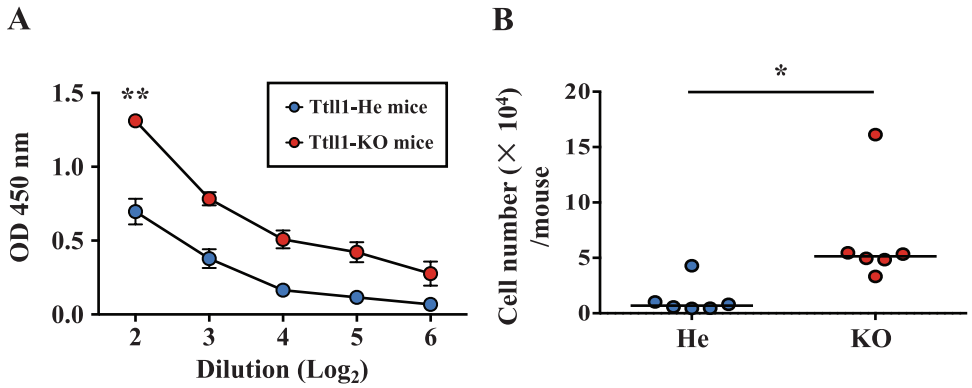

Fig. 1. PspA-specific nasal IgA immune responses in Ttll1-KO mice. Ttll1-He and Ttll1-KO mice were intra-nasally immunized with PspA and CT once weekly for 3 weeks. One week after the last immunization, PspA-specific nasal IgA immune responses were examined. (A) PspA-specific IgA in nasal wash was detected by ELISA. Ttll1-He, $n = 3$; Ttll1-KO, $n = 3$. Data are presented as means ± SEM and are representative of three independent experiments. $^{**}P < 0.01$ (Welch's *t*-test). OD, optical density. (B) Cells were isolated from the NPs and PspA-specific IgA-producing plasma cells were analyzed by ELISpot. Data are combined from two independent experiments; each point represents data from an individual mouse. The horizontal line indicates the mean in each group. $^{*}P < 0.05$ (Mann–Whitney *U*-test).

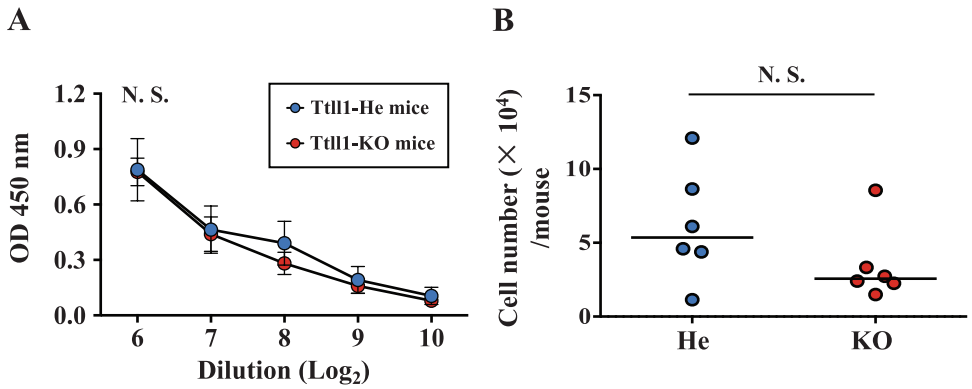

Fig. 2. CT-specific nasal IgA immune responses in Ttll1-KO mice. Ttll1-He and Ttll1-KO mice were intra-nasally immunized with PspA and CT once a week for 3 weeks. One week after the last immunization, (A) CT-specific IgA in nasal wash was detected by ELISA. Ttll1-He, $n = 3$; Ttll1-KO, $n = 3$. Data are presented as means ± SEM and are representative of three independent experiments. N.S., not significant (Welch's *t*-test); OD, optical density. (B) Cells were isolated from NPs and CT-specific IgA-producing plasma cells were analyzed by ELISpot. Data are combined from two independent experiments; each point represents data from an individual mouse. The horizontal line indicates the mean in each group. N.S., not significant (Mann–Whitney *U*-test).

Antigen-specific serum IgG immune responses were not changed in Ttll1-KO mice

To examine whether antigen-specific systemic immune responses were changed by airway mucociliary dysfunction, we examined the amount of antigen-specific serum IgG in immunized Ttll1-He and -KO mice. Both the amount of PspA-specific serum IgG and the amount of CT-specific serum IgG were similar in Ttll1-KO mice when compared with Ttll1-He mice (Fig. 3A, $P = 0.12$; Fig. 3B, $P = 0.11$), indicating that antigen-specific serum IgG immune responses were not changed by airway mucociliary dysfunction.

Mucus removal had little effect on the antigen-specific nasal IgA immune responses

To investigate whether mucus accumulation was involved in the higher immune responses to PspA in the respiratory mucosa of Ttll1-KO mice, we removed the dense mucus by using *N*-acetylcysteine, a clinically used mucolytic drug. In mice with mucus removed, both the amount of PspA-specific IgA in nasal wash and the number of PspA-specific IgA-producing plasma cells were significantly higher in the Ttll1-KO mice than in the Ttll1-He mice (Fig. 4A, $P < 0.001$; Fig. 4B, $P = 0.001$), and the amount of CT-specific IgA in nasal wash and the number of CT-specific IgA-producing plasma cells in Ttll1-KO mice were similar to those in Ttll1-He mice (Fig. 4C, $P = 0.41$; Fig. 4D, $P = 0.56$). These results indicate that the accumulated nasal mucus of Ttll1-KO mice was not involved in the enhanced immune responses to PspA.

Different retention and uptake patterns of PspA and CT in NALT

We then examined the underlying mechanisms of enhanced PspA-specific nasal IgA immune response in Ttll1-KO mice. We first asked whether the number of NALT M cells was affected by Ttll1 deficiency. To address this issue, we performed whole-mount staining of the murine

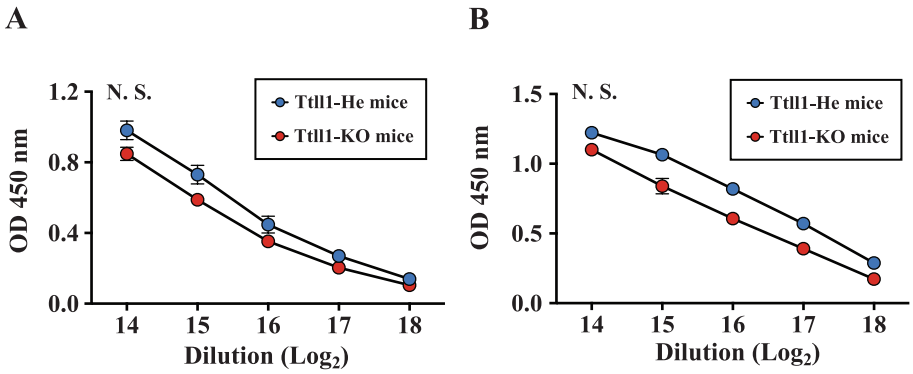

Fig. 3. Antigen-specific serum IgG immune responses in Ttll1-KO mice. Ttll1-He and Ttll1-KO mice were intra-nasally immunized with PspA and CT once weekly for 3 weeks. One week after the last immunization, PspA-specific (A) and CT-specific (B) IgG in serum were detected by ELISA. Ttll1-He, $n = 4$; Ttll1-KO, $n = 3$. Data are presented as means ± SEM and are representative of three independent experiments. N.S., not significant (Welch's *t*-test); OD, optical density.

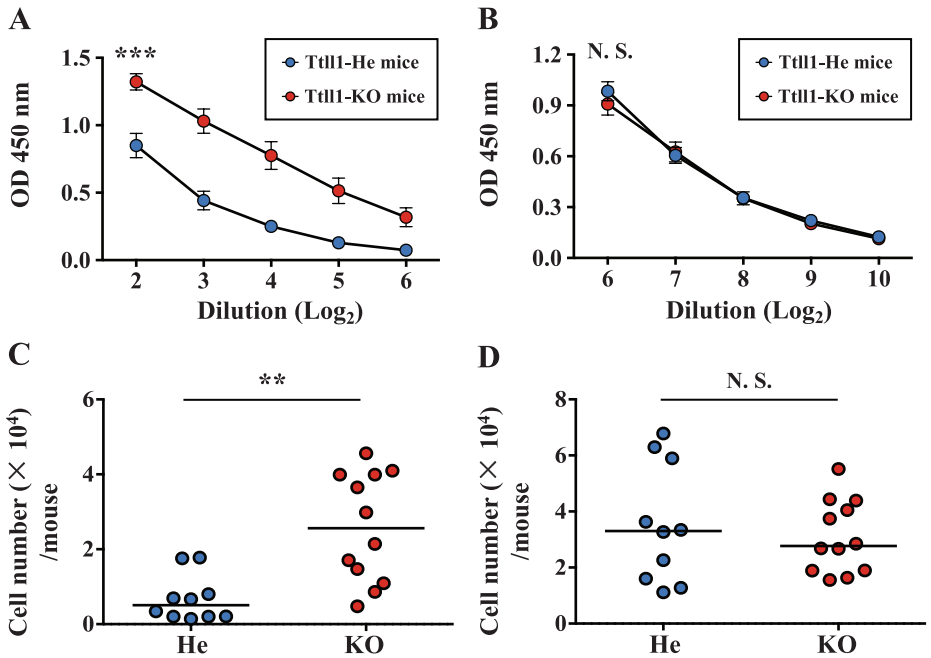

Fig. 4. Effect of mucus removal on the antigen-specific nasal IgA immune responses. Ttll1-He and Ttll1-KO mice were treated with *N*-acetylcysteine to remove nasal mucus and then intra-nasally immunized with PspA and CT. PspA-specific (A) and CT-specific (B) IgA in nasal wash were detected by ELISA. Data are presented as means ± SEM. Ttll1-He, $n = 7$; Ttll1-KO, $n = 9$. $^{***}P < 0.001$; N.S., not significant (Welch's *t*-test); OD, optical density. PspA-specific (C) and CT-specific (D) nasal IgA-producing plasma cells from NPs were analyzed by ELISpot. Data are combined from three independent experiments; each point represents data from an individual mouse. The horizontal line indicates the mean in each group. $^{**}P < 0.01$; $^{***}P < 0.001$; N.S., not significant (Mann–Whitney *U*-test).

palate, and found that the number of NALT M cells was not changed in Ttll1-KO mice when compared with Ttll1-He mice (Supplementary Figure 2). We next asked whether M cell function of antigen uptake was influenced by Ttll1 deficiency. To address this possibility, mice were intra-nasally administrated *N*-acetylcysteine to remove nasal mucus and then intra-nasally immunized with PspA. Immunohistological analysis indicated that uptake of PspA by NALT M cells not changed in Ttll1-KO mice when compared with Ttll1-He mice (Supplementary Figure 3). These results indicated that the number and function of NALT M cells were not influenced by Ttll1 deficiency.

We next examined whether antigen distribution or retention was changed in Ttll1-KO mice because of the impaired function of mucocillia. To address this issue, mice were intra-nasally immunized with biotinylated PspA and CT. According to histological analysis, high levels of PspA were detected in the NALT of Ttll1-He mice at 1 h after administration; this signal disappeared at 12 h after administration (Fig. 5A). In contrast, the PspA signal remained at 12 h after administration in Ttll1-KO mice (Fig. 5A).

Then, the distribution and retention time of CT were checked. In contrast to PspA, the CT signal did not disappear and remained on the NALT epithelium of both Ttll1-He and

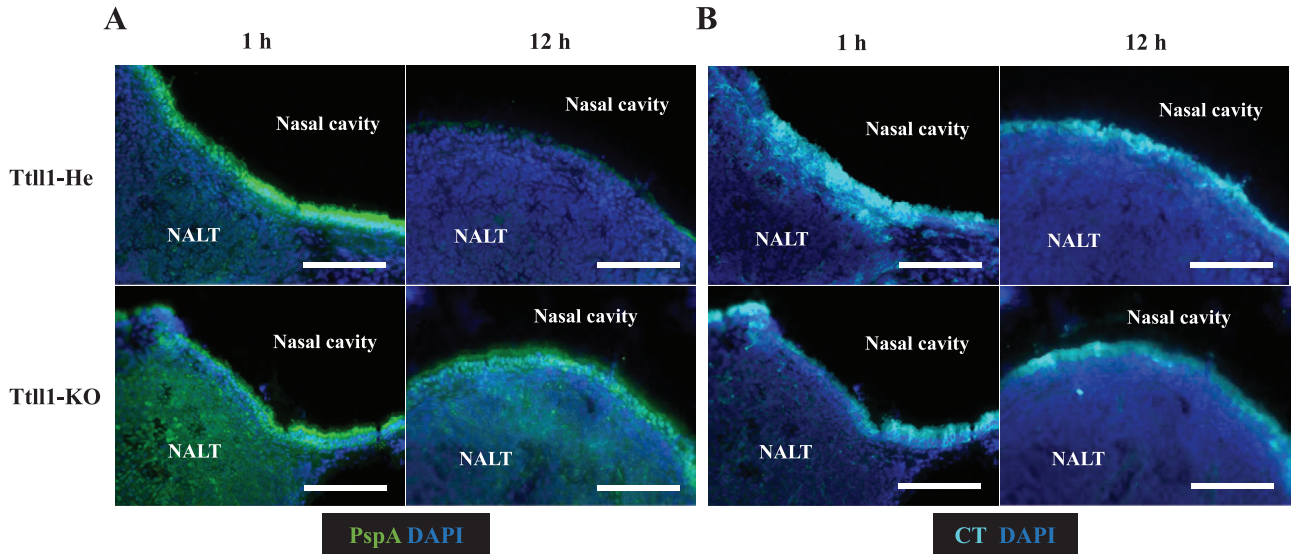

Fig. 5. Retention time of PspA and CT in the NALT of Ttll1-KO mice. Ttll1-He and Ttll1-KO mice were intra-nasally immunized with biotinylated PspA and CT to examine the distribution of PspA (A) and CT (B). NALT samples were taken at 1 h and 12 h after immunization. Frozen sections (6 μm) were stained with the indicated antibodies. Data are representative of two independent experiments, each with four Ttll1-He mice and five Ttll1-KO mice. Scale bars: 100 μm.

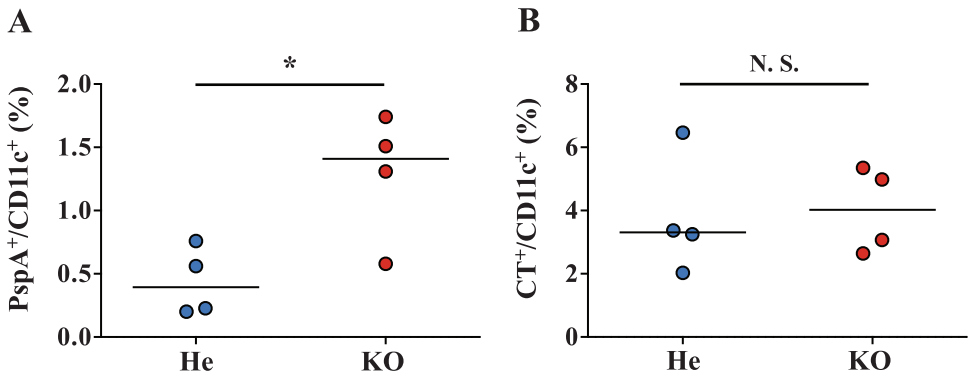

Fig. 6. Uptake of PspA and CT by DCs in the NALT of Ttll1-KO mice. Ttll1-He and Ttll1-KO mice were intra-nasally immunized with FITC-PspA and AF647-CT to detect the PspA (A) and CT (B) uptake. Cells were isolated from NALT at 12 h after immunization and analyzed by flow cytometry. Data are representative of two independent experiments; each point represents data from an individual mouse. The horizontal line indicates the mean in each group. *$P < 0.05$; N.S., not significant (Mann–Whitney *U*-test).

-KO mice at 12 h (Fig. 5B). These results show that PspA retention was prolonged in the NALT of Ttll1-KO mice, whereas CT retention was comparable between Ttll1-He and -KO mice, which is consistent with the results for antigen-specific nasal IgA immune responses.

Next, antigen uptake by DCs was examined by flow cytometry. Mice were intra-nasally immunized with FITC-PspA and AF647-CT, and cells were isolated from NALT at 12 h after administration. Consistent with the antigen retention data, we found that the percentage of $PspA^+$ cells in $CD11c^+$ DCs was significantly higher in Ttll1-KO mice than in Ttll1-He mice (Fig. 6A, $P = 0.025$), whereas the percentage of CT^+ cells in $CD11c^+$ DCs was comparable between Ttll1-He and -KO mice (Fig. 6B, $P = 0.85$). These results collectively indicate that the higher DC uptake of PspA in NALT of Ttll1-KO mice was caused by the prolonged PspA retention, and the lack of change in CT uptake was due to the lack of change in CT retention. Consequently, the different antigen-specific nasal IgA immune responses were induced by the different efficacy of DC uptake of antigen in the NALT.

Discussion

In this study, we demonstrated an enhanced PspA-specific nasal immune response in Ttll1-KO mice compared with Ttll1-He mice. We believe this difference was due to prolonged retention of the antigen on the NALT epithelium and higher uptake by DCs in the Ttll1-KO mice. Unexpectedly, the Ttll1-He mice and Ttll1-KO mice showed equal levels of CT-specific nasal IgA immune responses likely because the retention time of CT was longer than that of PspA in Ttll1-He mice: at 12 h after administration, PspA was cleared from the NALT epithelium, whereas some CT remained in Ttll1-He mice.

The different kinetics of the distribution of PspA and CT indicate that mucociliary clearance efficiently removed PspA, but not CT. Cilia beat asymmetrically in metachronal waves to propel pathogens and inhaled materials out of the airways. Because the ciliary asymmetric beating was impaired in Ttll1-KO mice but not Ttll1-He mice, PspA could persist on the NALT epithelium for longer in Ttll1-KO mice. Unlike PspA, CT has high affinity to the ganglioside GM1, which is widely distributed on the plasma membrane surface of various animal epithelial cells (38). We propose that the GM1 anchoring of CT to the NALT epithelial surface meant that normal ciliary beating could not remove CT from the airway in Ttll1-He mice. The higher PspA retention and uptake in the NALT of Ttll1-KO mice led to enhanced PspA-specific nasal IgA immune responses in these mice, whereas the similar levels of CT retention and intake between Ttll1-He and Ttll1-KO mice led to comparable CT-specific nasal IgA immune responses between these mice.

We previously showed that specific nasal IgA immune responses were reduced in Ttll1-KO mice compared with -He mice when mice were nasally immunized with PspA-C-CPE (35). Because airway mucus usually serves as a barrier to direct exposure to foreign materials, it is plausible that the accumulated nasal mucus in Ttll1-KO mice interrupts the approach of vaccine antigen to NALT epithelium. Consistent with this notion, binding of PspA-C-CPE to NALT was prevented by the thick mucus in the Ttll1-KO mice (35). However, when Ttll1-KO mice were immunized with PspA and CT, neither PspA-specific nor CT-specific nasal IgA immune responses were impaired, suggesting that the thick mucus layer did not prevent the binding of PspA or CT to NALT epithelium. Therefore, the characteristics of different proteins might play critical roles in their ability to reach and bind to the epithelium. Indeed, when we intra-nasally administrated mice with PspA alone, we found that the binding of PspA to NALT epithelium was detected in Ttll1-He mice, but not in Ttll1-KO mice (Supplementary Figure 4A). In contrast, when we intra-nasally administrated mice with PspA together with CT, we detected the binding of PspA to NALT epithelium in both Ttll1-He mice and Ttll1-KO mice (Supplementary Figure 4B). These results indicated that CT was a critical factor which influences the binding of PspA to NALT epithelium in Ttll1-KO mice. A possible explanation of our results is that CT penetrated the mucus layer of Ttll1-KO mice and then disrupted the dense mucus layer by inducing fluid secretion, especially water secretion, which allowed the PspA to attach to the NALT epithelium without interference. Supporting this notion, it is reported that CT causes fluid secretion in the intestine and mechanically disrupts the mucus layer (39). CT plays important roles in the induction of mucosal immunity by inducing the differentiation of M-like cells in the intestinal villi (40), increasing permeability of intestinal epithelium (41) and facilitating antigen presentation by various types of APCs (42). In addition, CT induces the accumulation of cAMP in airway epithelial cells, which increases ciliary beating frequency and ciliary bend angle (43). However, the increased ciliary beating was not sufficient to recover the mucociliary dysfunction of Ttll1-KO mice. Ciliary beating is asymmetric, with clearly distinguished effective and recovery strokes. This asymmetry is crucial for mucociliary clearance and requires tubulin glutamylation (21). Our group's previous study of Ttll1 indicated that the beating frequency of Ttll1-KO mice is higher than that of wild-type mice, but Ttll1-KO mice have lost beating asymmetry (21). Therefore, even though it is likely that CT increased cAMP accumulation and thereby promoted ciliary beating, the mucociliary dysfunction of Ttll1-KO mice was not recovered; hence, PspA was not rapidly removed in Ttll1-KO mice.

Mucins cross-link in the mucus layer to form a selective fiber mesh. Therefore, protein size might dictate whether a protein can penetrate the mucus barrier. However, from structure analyses, we inferred that both CT (44) and PspA-C-CPE (45, 46) are smaller than the average pore size of the mesh (47). It is therefore necessary to consider other interactions, e.g. hydrophobicity, which can limit the diffusion of protein in mucus (48). Analysis of the α-helical domains of PspA and its amino acids sequence suggests that PspA is hydrophobic (49). C-CPE contains both hydrophobic and hydrophilic regions (44), but because PspA (~43 kDa) is much larger than C-CPE (~17.3 kDa), PspA-C-CPE is likely hydrophobic. CT is regarded as hydrophilic (50, 51) because the hydrophilic A2 subunit shields the hydrophobicity of the A1 subunit, and the A1 subunit is packed into the hydrophilic B subunit pentamer. Therefore, it is plausible that the mucus layer prevents penetration of PspA and PspA-C-CPE but not CT. Charge interactions can also limit the diffusion of proteins in mucus. Mucin fibers, which contain highly glycosylated segments, are negatively charged, and show high affinity with positively charged particles (52). PspA has an overall positive charge in the amino-terminal domain, which is exposed on the surface (53), although the claudin-4-binding site in C-CPE is negatively charged (54). Therefore, PspA and PspA-C-CPE are likely trapped by mucin fibers. Although the B subunit of CT carries a net negative charge (55), whole CT shows charge heterogeneity (44, 56); therefore, more studies are required to determine the charge interactions between CT and mucus.

In addition to antigen-specific IgA in NPs, antigen-specific IgG in serum plays an important role in preventing pathogenesis. Interestingly, unlike PspA-specific nasal IgA, the concentrations of PspA-specific IgG were comparable between Ttll1-He mice and Ttll1-KO mice. CT-specific serum IgG likewise showed no significant difference between Ttll1-He and Ttll1-KO mice. In addition to NALT, some other cell types and tissues are related to immune response induction in the respiratory tract. For instance, inducible bronchus-associated lymphoid tissue is induced by virus-based vaccine delivery, inflammation and infection, and initiates antigen-specific immune responses (57), and respiratory M cells in the respiratory epithelium function similarly to NALT by taking up vaccine antigens to induce antigen-specific systemic immune responses (58). Therefore, both inducible bronchus-associated lymphoid tissue and respiratory M cells are possible alternative pathways for the induction of PspA-specific IgG in both Ttll1-He and Ttll1-KO mice.

In summary, the fluid secretion induced by CT likely disrupted the dense mucus barrier of Ttll1-KO mice and made it possible for PspA to access the NALT epithelium. Furthermore, the impaired ciliary clearance in the Ttll1-KO mice extended the PspA retention thereby enhancing the PspA-specific nasal IgA immune responses. Various adjuvants, in addition to CT,

have been used in mucosal vaccine development. Because these adjuvants display different characteristics it would be interesting to investigate their relationship with the physical barriers of mucus layer and cilia. Taken together, this study provides evidence that mucociliary function, which removes vaccine antigen from the NALT epithelium, is a critical factor in the efficacy of nasal vaccines. Therefore, temporal control of the function of respiratory cilia would be a useful strategy for development of efficient nasal vaccines.

Funding

This work was supported by the Ministry of Education, Culture, Sports, Science and Technology of Japan (MEXT)/Japan Society for the Promotion of Science KAKENHI (grant numbers JP15H05790, JP18H02150, JP18H02674 and JP17K09604 to J.K.; JP18K17997 to K.H.); the Japan Agency for Medical Research and Development (AMED; JP17fk0108223h0002, JP17ak0101068h0001, JP17gm1010006s0101, 19ek0410062h0001 and 20fk0108145h0001 to J.K.); the Ministry of Health, Labour and Welfare of Japan (JP19KA3001 to K.H.); the Science and Technology Research Promotion Program for Agriculture, Forestry, Fisheries, and Food Industry (to J.K.); a grant-in-aid for Scientific Research on Innovative Areas from MEXT (JP23116506, JP16H01373 and JP25116706 to J.K.); the Grant for Joint Research Project of the Institute of Medical Science, the University of Tokyo (to J.K.), the Ono Medical Research Foundation (to J.K.); and the Canon Foundation (to J.K.).

Conflicts of interest statement: the authors declared no conflicts of interest.

References

1 Fukuyama, Y., King, J. D., Kataoka, K. *et al.* 2010. Secretory-IgA antibodies play an important role in the immunity to *Streptococcus pneumoniae*. *J. Immunol.* 185:1755.
2 Miquel-Clopés, A., Bentley, E. G., Stewart, J. P. and Carding, S. R. 2019. Mucosal vaccines and technology. *Clin. Exp. Immunol.* 196:205.
3 Kiyono, H. and Azegami, T. 2015. The mucosal immune system: from dentistry to vaccine development. *Proc. Jpn. Acad. Ser. B Phys. Biol. Sci.* 91:423.
4 Kunisawa, J., Nochi, T. and Kiyono, H. 2008. Immunological commonalities and distinctions between airway and digestive immunity. *Trends Immunol.* 29:505.
5 Yuki, Y. and Kiyono, H. 2003. New generation of mucosal adjuvants for the induction of protective immunity. *Rev. Med. Virol.* 13:293.
6 Kelsall, B. L. and Strober, W. 1996. Distinct populations of dendritic cells are present in the subepithelial dome and T cell regions of the murine Peyer's patch. *J. Exp. Med.* 183:237.
7 Mora, J. R., Iwata, M., Eksteen, B. *et al.* 2006. Generation of gut-homing IgA-secreting B cells by intestinal dendritic cells. *Science* 314:1157.
8 Kunisawa, J., Nakanishi, T., Takahashi, I. *et al.* 2001. Sendai virus fusion protein mediates simultaneous induction of MHC class I/II-dependent mucosal and systemic immune responses via the nasopharyngeal-associated lymphoreticular tissue immune system. *J. Immunol.* 167:1406.
9 Yamamoto, M., McGhee, J. R., Hagiwara, Y., Otake, S. and Kiyono, H. 2001. Genetically manipulated bacterial toxin as a new generation mucosal adjuvant. *Scand. J. Immunol.* 53:211.
10 Xu-Amano, J., Kiyono, H., Jackson, R. J. *et al.* 1993. Helper T cell subsets for immunoglobulin A responses: oral immunization with tetanus toxoid and cholera toxin as adjuvant selectively induces Th2 cells in mucosa associated tissues. *J. Exp. Med.* 178:1309.
11 Marinaro, M., Staats, H. F., Hiroi, T. *et al.* 1995. Mucosal adjuvant effect of cholera toxin in mice results from induction of T helper 2 (Th2) cells and IL-4. *J. Immunol.* 155:4621.
12 Lycke, N. and Strober, W. 1989. Cholera toxin promotes B cell isotype differentiation. *J. Immunol.* 142:3781.
13 Lai, S. K., Wang, Y. Y., Wirtz, D. and Hanes, J. 2009. Micro- and macrorheology of mucus. *Adv. Drug Deliv. Rev.* 61:86.
14 Williams, O. W., Sharafkhaneh, A., Kim, V., Dickey, B. F. and Evans CM. 2006. Airway mucus. *Am. J. Respir. Cell Mol. Biol.* 34:527.
15 Li, Y., Bharti, A., Chen, D., Gong, J. and Kufe, D. 1998. Interaction of glycogen synthase kinase 3β with the DF3/MUC1 carcinoma-associated antigen and β-catenin. *Mol. Cell Biol.* 18:7216.
16 Carraway, K. L., Perez, A., Idris, N. *et al.* 2002. Muc4/sialomucin complex, the intramembrane ErbB2 ligand, in cancer and epithelia: to protect and to survive. *Prog. Nucleic Acid Res. Mol. Biol.* 71:149.
17 Moniaux, N., Escande, F., Batra, S. K., Porchet, N., Laine, A. and Aubert, J. P. 2000. Alternative splicing generates a family of putative secreted and membrane-associated MUC4 mucins. *Eur. J. Biochem.* 267:4536.
18 Sheehan, J. K., Kirkham, S., Howard, M. *et al.* 2004. Identification of molecular intermediates in the assembly pathway of the MUC5AC mucin. *J. Biol. Chem.* 279:15698.
19 Chilvers, M. A. and O'Callaghan, C. 2000. Local mucociliary defence mechanisms. *Paediatr. Respir. Rev.* 1:27.
20 Janke, C., Rogowski, K., Wloga, D. *et al.* 2005. Tubulin polyglutamylase enzymes are members of the TTL domain protein family. *Science* 308:1758.
21 Ikegami, K., Sato, S., Nakamura, K., Ostrowski, L. E. and Setou, M. 2010. Tubulin polyglutamylation is essential for airway ciliary function through the regulation of beating asymmetry. *Proc. Natl Acad. Sci. USA* 107:10490.
22 Grevers, G.; First International Roundtable ENT Meeting Group. 2010. Challenges in reducing the burden of otitis media disease: an ENT perspective on improving management and prospects for prevention. *Int. J. Pediatr. Otorhinolaryngol.* 74:572.
23 Miyaji, E. N., Oliveira, M. L., Carvalho, E. and Ho, P. L. 2013. Serotype-independent pneumococcal vaccines. *Cell. Mol. Life Sci.* 70:3303.
24 Park, I. H., Pritchard, D. G., Cartee, R., Brandao, A., Brandileone, M. C. and Nahm, M. H. 2007. Discovery of a new capsular serotype (6C) within serogroup 6 of *Streptococcus pneumoniae*. *J. Clin. Microbiol.* 45:1225.
25 Calix, J. J. and Nahm, M. H. 2010. A new pneumococcal serotype, 11E, has variably inactivated wcjE gene. *J. Infect. Dis.* 202:29.
26 Daniels, C. C., Rogers, P. D. and Shelton, C. M. 2016. A review of pneumococcal vaccines: current polysaccharide vaccine recommendations and future protein antigens. *J. Pediatr. Pharmacol. Ther.* 21:27.
27 Richter, S. S., Heilmann, K. P., Dohrn, C. L., Riahi, F., Diekema, D. J. and Doern, G. V. 2013. Pneumococcal serotypes before and after introduction of conjugate vaccines, United States, 1999–2011. *Emerg. Infect. Dis.* 19:1074.
28 Hsu, H. E., Shutt, K. A., Moore, M. R. *et al.* 2009. Effect of pneumococcal conjugate vaccine on pneumococcal meningitis. *N. Engl. J. Med.* 360:244.
29 Crain, M. J., Waltman, W. D., Turner, J. S. *et al.* 1990. Pneumococcal surface protein A (PspA) is serologically highly variable and is expressed by all clinically important capsular serotypes of *Streptococcus pneumoniae*. *Infect. Immun.* 58:3293.
30 Moreno, A. T., Oliveira, M. L., Ferreira, D. M. *et al.* 2010. Immunization of mice with single PspA fragments induces antibodies capable of mediating complement deposition on different pneumococcal strains and cross-protection. *Clin. Vaccine Immunol.* 17:439.
31 Yamamoto, M., Briles, D. E., Yamamoto, S., Ohmura, M., Kiyono, H. and McGhee, J. R. 1998. A nontoxic adjuvant for mucosal immunity to pneumococcal surface protein A. *J. Immunol.* 161:4115.
32 Suzuki, H., Watari, A., Hashimoto, E. *et al.* 2015. C-terminal *Clostridium perfringens* enterotoxin-mediated antigen delivery for nasal pneumococcal vaccine. *PLoS One* 10:e0126352.
33 Tada, R., Suzuki, H., Takahashi, S. *et al.* 2018. Nasal vaccination with pneumococcal surface protein A in combination with

cationic liposomes consisting of DOTAP and DC-chol confers antigen-mediated protective immunity against *Streptococcus pneumoniae* infections in mice. *Int. Immunopharmacol.* 61:385.
34 Kakutani, H., Kondoh, M., Fukasaka, M., Suzuki, H., Hamakubo, T. and Yagi, K. 2010. Mucosal vaccination using claudin-4-targeting. *Biomaterials* 31:5463.
35 Suzuki, H., Nagatake, T., Nasu, A. *et al.* 2018. Impaired airway mucociliary function reduces antigen-specific IgA immune response to immunization with a claudin-4-targeting nasal vaccine in mice. *Sci. Rep.* 8:2904.
36 Barthelson, R., Mobasseri, A., Zopf, D. and Simon, P. 1998. Adherence of *Streptococcus pneumoniae* to respiratory epithelial cells is inhibited by sialylated oligosaccharides. *Infect. Immun.* 66:1439.
37 Rayner, C. F., Jackson, A. D., Rutman, A. *et al.* 1995. Interaction of pneumolysin-sufficient and -deficient isogenic variants of *Streptococcus pneumoniae* with human respiratory mucosa. *Infect. Immun.* 63:442.
38 van Ginkel, F. W., Jackson, R. J., Yuki, Y. and McGhee, J. R. 2000. Cutting edge: the mucosal adjuvant cholera toxin redirects vaccine proteins into olfactory tissues. *J. Immunol.* 165:4778.
39 Guichard, A., Cruz-Moreno, B., Cruz-Moreno, B. C. *et al.* 2013. Cholera toxin disrupts barrier function by inhibiting exocyst-mediated trafficking of host proteins to intestinal cell junctions. *Cell Host Microbe* 14:294.
40 Terahara, K., Yoshida, M., Igarashi, O. *et al.* 2008. Comprehensive gene expression profiling of Peyer's patch M cells, villous M-like cells, and intestinal epithelial cells. *J. Immunol.* 180:7840.
41 Lycke, N., Karlsson, U., Sjölander, A. and Magnusson, K. E. 1991. The adjuvant action of cholera toxin is associated with an increased intestinal permeability for luminal antigens. *Scand. J. Immunol.* 33:691.
42 Holmgren, J., Lycke, N. and Czerkinsky, C. 1993. Cholera toxin and cholera B subunit as oral-mucosal adjuvant and antigen vector systems. *Vaccine* 11:1179.
43 Kogiso, H., Hosogi, S., Ikeuchi, Y. *et al.* 2018. [Ca2+]i modulation of cAMP-stimulated ciliary beat frequency via PDE1 in airway ciliary cells of mice. *Exp. Physiol.* 103:381.
44 Zhang, R. G., Scott, D. L., Westbrook, M. L. *et al.* 1995. The three-dimensional crystal structure of cholera toxin. *J. Mol. Biol.* 251:563.
45 Senkovich, O., Cook, W. J., Mirza, S. *et al.* 2007. Structure of a complex of human lactoferrin N-lobe with pneumococcal surface protein a provides insight into microbial defense mechanism. *J. Mol. Biol.* 370:701.
46 Shinoda, T., Shinya, N., Ito, K. *et al.* 2016. Structural basis for disruption of claudin assembly in tight junctions by an enterotoxin. *Sci. Rep.* 6:33632.
47 Duncan, G. A., Jung, J., Hanes, J. and Suk, J. S. 2016. The mucus barrier to inhaled gene therapy. *Mol. Ther.* 24:2043.
48 Lai, S. K., Wang, Y.-Y. and Hanes, J. 2009. Mucus-penetrating nanoparticles for drug and gene delivery to mucosal tissues. *Adv. Drug Deliv. Rev.* 61:158.
49 Yun, K. W., Choi, E. H. and Lee, H. J. 2017. Genetic diversity of pneumococcal surface protein A in invasive pneumococcal isolates from Korean children, 1991–2016. *PLoS One* 12:e0183968.
50 Ward, W. H., Britton, P. and van Heyningen, S. 1981. The hydrophobicities of cholera toxin, tetanus toxin and their components. *Biochem. J.* 199:457.
51 Yamamoto, T., Nakazawa, T., Miyata, T., Kaji, A. and Yokota, T. 1984. Evolution and structure of two ADP-ribosylation enterotoxins, *Escherichia coli* heat-labile toxin and cholera toxin. *FEBS Lett.* 169:241.
52 Liu, M., Zhang, J., Shan, W. and Huang, Y. 2015. Developments of mucus penetrating nanoparticles. *Asian J. Pharm. Sci.* 10:275.
53 Yother, J., Handsome, G. L. and Briles, D. E. 1992. Truncated forms of PspA that are secreted from *Streptococcus pneumoniae* and their use in functional studies and cloning of the pspA gene. *J. Bacteriol.* 174:610.
54 Kimura, J., Abe, H., Kamitani, S. *et al.* 2010. *Clostridium perfringens* enterotoxin interacts with claudins via electrostatic attraction. *J. Biol. Chem.* 285:401.
55 Leitch, J. J., Brosseau, C. L., Roscoe, S. G., Bessonov, K., Dutcher, J. R. and Lipkowski, J. 2013. Electrochemical and PM-IRRAS characterization of cholera toxin binding at a model biological membrane. *Langmuir* 29:965.
56 Kabir, S. 1986. Charge heterogeneity of cholera toxin and its subunits. *FEMS Microbiol. Lett.* 37:155.
57 Nagatake, T., Suzuki, H., Hirata, S. I. *et al.* 2018. Immunological association of inducible bronchus-associated lymphoid tissue organogenesis in Ag85B-rHPIV2 vaccine-induced anti-tuberculosis mucosal immune responses in mice. *Int. Immunol.* 30:471.
58 Kim, D. Y., Sato, A., Fukuyama, S. *et al.* 2011. The airway antigen sampling system: respiratory M cells as an alternative gateway for inhaled antigens. *J. Immunol.* 186:4253.